Solute Transport through Unsteady Hydrologic Systems Along a Plug Flow-to-Uniform Sampling Continuum

Stanley B. Grant[1,2], **Ciaran J. Harman**[3,4]

[1]Occoquan Watershed Monitoring Laboratory, The Charles E. Via, Jr. Department of Civil and Environmental Engineering, Virginia Tech, 9408 Prince William Street, Manassas VA 20110

[2]Center for Coastal Studies, Virginia Tech, 1068A Derring Hall (0420), Blacksburg, VA 24061

[3]Department of Environmental Health and Engineering, Johns Hopkins University, Baltimore, MD, USA

[4]Department of Earth and Planetary Science, Johns Hopkins University, Baltimore, MD, USA

Key Points:

- formulae are derived for age-ranked storage in, and solute transport through, unsteady hydrologic systems under shifted-uniform selection
- the SAS function's single parameter indicates where a system falls along a continuum between plug-flow and uniform sampling
- model predictions are concordant with published measurements of solute breakthrough in a sloping lysimeter subject to periodic wetting

Corresponding author: Stanley B. Grant, `stanleyg@vt.edu`

Abstract

Unsteady transit time distribution (TTD) theory is a promising new approach for merging hydrologic and water quality models at the catchment scale. A major obstacle to widespread adoption of the theory, however, has been the specification of the StorAge Selection (SAS) function, which describes how the selection of water for outflow is biased by age. In this paper we hypothesize that some unsteady hydrologic systems of practical interest can be described, to first-order, by a "shifted-uniform" SAS that falls along a continuum between plug flow sampling (for which only the oldest water in storage is sampled for outflow) and uniform sampling (for which water in storage is sampled randomly for outflow). For this choice of SAS function, explicit formulae are derived for the evolving: (1) age distribution of water in storage; (2) age distribution of water in outflow; and (3) breakthrough concentration of a conservative solute under either continuous or impulsive addition. Model predictions conform closely to chloride and deuterium breakthrough curves measured previously in a sloping lysimeter subject to periodic wetting, although refinements of the model are needed to account for the reconfiguration of flow paths at high storage levels (the so-called inverse storage effect). The analytical results derived in this paper should lower the barrier to applying TTD theory in practice, ease the computational demands associated with simulating solute transport through complex hydrologic systems, open up new opportunities for real-time control, and provide physical insights that might not be apparent from traditional numerical solutions of the governing equations.

Plain Language Summary

Many hydrologic systems, from hillslopes to water distribution systems, are intrinsically unsteady, by which we mean the flow of water and solutes varies continuously as a function of time. Historically, water quality models of such systems start by resolving the unsteady flow field first, and then "layering on" mass conservation laws in one-, two- or three-dimensions. A promising new approach, unsteady transit time distribution (TTD) theory, takes an entirely different tack, by tracking the flux and age distribution of water and solute moving into and out of a control volume drawn around the system of interest. Practical implementation of the theory requires choosing a storAge selection (SAS) function appropriate for the system under study. In this paper we propose a SAS function, which we call a "shifted-uniform SAS", that captures a continuum of physical be-

havior and thus may provide a first-order description of many natural and engineered hydrologic systems. This choice of SAS function also leads to data-tested formulae for predicting water quality outcomes.

1 Introduction

Transit Time Distribution (TTD) theory elegantly addresses many long-standing challenges associated with modeling solute transport through complex and heterogeneous hydrologic systems (Kirchner (2016)). Recently the theory has been extended to rigorously account for unsteady flow, and the consequent temporal evolution of TTDs, through the use of StorAge Selection (SAS) functions (Botter et al. (2011), Rinaldo et al. (2015)). This new approach is typically implemented in five steps: (1) a control volume is drawn around the system of interest (e.g., the vadose zone in Figure (1a)); (2) an unsteady water balance is performed over the control volume accounting for inflows, $J(t)$ [L T^{-1}], discharge and evapotranspiration, $Q(t)$ and $ET(t)$ [L T^{-1}] and the change of water volume in storage, $S(t)$ [L], over time t (note that all flows and volumes are normalized by the surface area of the system); (3) a SAS function (i.e., a probability distribution and its parameters) is chosen to approximate how water selected from storage for outflow is biased by age; (4) the age conservation equation (ACE) is solved to yield the age distributions of water in storage and outflow; and (5) the solute concentration leaving the control volume, $C_Q(t)$ [M L^{-3}], is calculated from these preceding results, by convolving the time history of inflow solute concentration, $C_J(t)$ [M L^{-3}], with the age distribution of water in outflow, after accounting for any age-dependent reactions.

Key strengths of this transient version of TTD theory include its conceptual simplicity, parsimony and the relative ease with which the theory can be upscaled to natural catchments (Rodriguez et al. (2018)). A significant challenge, at present, is the selection of the SAS function (step 3). This function, which gives the fraction of outflow drawn from each age-ranked volume-increment of water in storage, is an emergent property of the physics underlying water and solute transport through the control volume. In principal, the SAS function can be evaluated by volume averaging the advection-dispersion equation, although such an approach is practical only for the simplest of flow fields; e.g., one-dimensional, uniform and steady-state advection (Benettin et al. (2013)). In practice, one of several flexible parameterized probability distributions are often adopted, such as the uniform, Dirac delta (for plug-flow), Beta, or Gamma distributions (Hrachowitz

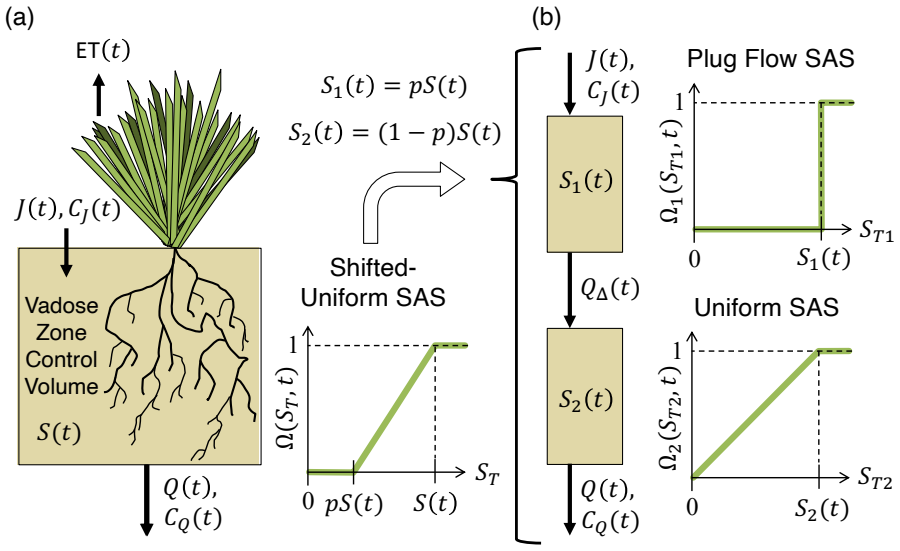

Figure 1: Application of transient TTD Theory to unsteady solute transport through a control volume drawn around the vadose zone. (a) All water balance terms ($J(t)$, $Q(t)$, $ET(t)$, and $S(t)$) and solute concentrations ($C_J(t)$ and $C_Q(t)$) vary with time. Unsteady solute transport through the vadose zone is assumed to follow a shifted uniform SAS function, $\Omega(S_T(t), t)$, expressed here as a CDF, where p is the system-specific percentile of age-ranked storage that is not sampled for outflow. (b) The system illustrated in (a) can be represented equivalently by two tanks in series of volumes $S_1(t) = pS(t)$ and $S_2(t) = (1 - p)S(t)$, respectively. Water leaves the first tank by plug flow sampling ($\Omega_1(S_{T1}(t), t)$), while water leaves the second tank by uniform sampling ($\Omega_2(S_{T2}(t), t)$). The transfer of water volume between tanks is represented by the variable Q_Δ. In this first implementation of the theory, water leaves the vadose zone by discharge only (i.e., $ET(t) = 0$).

et al. (2016)). A major impediment to the broad application of TTD theory is the absence of a general framework for selecting the SAS function that best represents solute transport through a particular hydrologic system.

Here we propose and discuss a SAS functional form that has the advantages of being: (1) parsimonious (it has only one free parameter); (2) able to capture key emergent structural properties of certain hydrologic systems; (3) solvable analytically in terms of simple integrals of the time-varying fluxes and storage; and (4) a generalization to transient conditions of commonly-assumed steady-state transit time distributions. This new

functional form, which we call a shifted-uniform SAS, is capable of representing mass transport along a continuum from pure plug flow sampling (for which only the oldest water in storage is selected for outflow) to pure random or "uniform" sampling (for which all water in storage has an equal probability of being selected for outflow regardless of its age). These two end-members represent conceptual limits for solute transport by, respectively, advection (plug flow sampling) or dispersive spreading (uniform sampling). Because advection and dispersive spreading are universal controls on solute transport through environmental matrices, we hypothesize that many unsteady hydrologic systems can be situated along a continuum between these two limits. The fact that our analysis yields explicit solutions for the evolving age structure of water in storage and outflow, as well as solute breakthrough concentration, lowers the barrier to applying the theory in practice, opens up the possibility of real-time control of non-linear hydrologic systems (Haber et al. (2021)), and provides physical insights that might not be apparent from numerical solutions alone.

As a first test, we apply the framework to a canonical problem in unsteady hydrology: solute transport through a vadose zone above a perched water table. Predictive models of solute transport through such systems must contend with extreme temporal and spatial variability in flow and soil saturation, arising from the stochastic nature of water movement into the vadose zone during rain events, the unsteady transfer of water out of the vadose zone by evapotranspiration and discharge, and the three-dimensional nature of internal flow paths (Simunek et al. (2008), Parker et al. (2021)). We demonstrate that a shifted-uniform representation of such systems is mathematically equivalent two storage zones or tanks arranged in series. The first tank is assigned a plug-flow SAS to represent the unsteady advection of solutes along the fastest flow paths through a system (e.g., due to soil piping (Hester and Fox (2020))). The second tank is assigned a uniform SAS to capture the spreading and dilution of solutes by geomorphic dispersion (associated with large-scale variations in the flow field along with variability in where solutes enters the system (Rinaldo et al. (1991))) and kinematic or mechanical dispersion (associated with pore-scale variations in the flow field (Botter and Rinaldo (2003))). The model's single parameter indicates the partitioning of storage volume between the two tanks, and thus determines where along the plug flow-to-uniform SAS continuum a particular hydrologic system falls.

The paper is organized as follows. In Section 2 we demonstrate that the shifted-uniform SAS is mathematically equivalent to two-tanks in series, and use this insight to solve the underlying age conservation equations analytically, leading to explicit formulae for the age structure of water in storage and outflow, as well as solute breakthrough under various assumptions about the nature of solute loading. In Section 3 the model's single parameter (reflecting the partitioning of storage volume between the two tanks) is inferred from previously published measurements of conservative tracer transport through a sloping lysimeter with a vadose zone and perched water table (Kim et al., 2018). Discussion and conclusions are presented in Sections 4 and 5, respectively.

2 Model Set-up and Solution

Following the steps outlined in the introduction, we begin by drawing a control volume around a portion of a vadose zone with a perched water table (Step 1) (Figure 1a). Water balance over the control volume (Step 2) is then determined by measuring inflows and outflows (as was done in the experiments described later) or by solving physics-based models of flow through transiently saturated porous media subject to rainfall forcing; e.g., by numerically solving the Richards equation and associated hydraulic relationships for unsteady flow through partially saturated porous media (Simunek et al. (2008)), and using the Penman-Monteith equation to estimate evapotranspiration from measurements of temperature, relative humidity, solar radiation and pressure deficit (Allen et al. (1998)). Outcomes of Step 2 include time series for $J(t)$, $ET(t)$, $Q(t)$, and $S(t)$.

The evolving age structure of water in the control volume is then estimated by solving the age conservation equation (ACE), where the dependent variable $S_T(T,t)$ [L T^{-1}], called the age-ranked storage function, is defined as the area-normalized volume of water in storage at time, t, with ages less than or equal to T:

$$\frac{\partial S_T}{\partial t} = J(t) - Q(t)P_Q(T,t) - ET(t)P_{ET}(T,t) - \frac{\partial S_T}{\partial T} \tag{1a}$$

$$S_T(T=0,t) = 0 \tag{1b}$$

$$S_T(T,t=0) = S_0 H(T - T_0) \tag{1c}$$

$$H(x) = \begin{cases} 0, x < 0 \\ 1, x \geq 0 \end{cases} \tag{1d}$$

Mathematically, the age-ranked storage function can be written as the product of the area-normalized volume of water in storage, $S(t)$, and the cumulative distribution function (CDF) form of its age distribution or "residence time distribution", $P_{\mathrm{RTD}}(T,t)$: $S_T(T,t) = S(t) \times P_{\mathrm{RTD}}(T,t)$. As written here, the ACE equates the time rate of change of the age-ranked storage function (left hand side) to the inflow of water of age $T = 0$ (first term on right hand side); discharge of water by drainage and evapotranspiration with age distributions $P_Q(T,t)$ (second term) and $P_{ET}(T,t)$ (third term), respectively; and aging of water in storage (fourth term). The boundary condition ((equation (1b)) ensures that no water in storage has an age less than $T = 0$. The initial condition (equation (1c)) implies that, at time $t = 0$, all water in storage, S_0, has a single age, $T = T_0$. In general, the age distribution of this *original* water is unknown (and likely unknowable), but by mathematically tagging it with an age of $T = T_0$ we can evaluate how quickly the initial condition's influence on age-ranked storage fades away with time (as demonstrated below). The age distributions, $P_{\mathrm{RTD}}(T,t)$, $P_Q(T,t)$ and $P_{ET}(T,t)$, are all expressed as CDFs, and thus represent the fraction of water with age less than or equal to, T at time t in, respectively, storage, discharge, or ET. The function $H(\cdot)$ is a unit step or Heaviside function.

Equation (1a) is a single equation in three unknown functions: the age-ranked storage function, $S_T(T,t)$, and CDFs for the age distribution of water leaving the control volume by discharge and evapotranspiration, $P_Q(T,t)$ and $P_{ET}(T,t)$. This closure problem can be addressed by introducing a new CDF, the SAS function, $\Omega(S_T,t)$ [-]. The SAS function captures the physics of water and solute transport through unsteady hydrologic systems by mapping the fraction of discharge with ages less than or equal to T to the fraction of age-ranked water in storage with that age or younger selected for discharge: $P_Q(T,t) = \Omega_Q(S_T,t)$ and $P_{ET}(T,t) = \Omega_{ET}(S_T,t)$. Thus, before the ACE can be solved (Step 4 in the introduction), a SAS function appropriate to the system under study must be selected (Step 3). In this study we hypothesize that a SAS function for the vadose zone must capture two key physical processes: (1) younger water travels some (storage-dependent) distance through the system before it can be sampled for discharge; and (2) older water in the system is sampled more-or-less randomly by age, reflecting the various paths by which water can travel through a hydrologic system before arriving at the outlet. The shifted-uniform SAS function meets both requirements, where the fraction

$p \in [0,1]$ is the percentile of the youngest age-ranked storage not sampled for discharge:

$$P_Q(T,t) = \Omega(S_T,t) = H(S_T(T,t) - pS(t))\frac{S_T(T,t) - pS(t)}{(1-p)S(t)} \tag{2}$$

The value of p, which in general must be inferred (e.g., by fitting the model to measured solute breakthrough data, as described later), determines where a particular system falls along the continuum between pure uniform sampling ($p \to 0$) and pure plug flow sampling ($p \to 1$). In the next section we derive an exact solution for age-ranked storage under shifted-uniform selection, by representing the vadose zone as two tanks in series. Without loss of generality and for consistency with the experimental data presented later, in the analysis presented below we will assume that water leaves the vadose zone by drainage alone; i.e., evapotranspiration is neglected.

2.1 Age-Ranked Storage Under Shifted-Uniform Selection

2.1.1 Conceptualizing the Problem as Two Tanks-in-Series

The shifted-uniform SAS function can be represented conceptually and mathematically as two tanks in series (Figure 1b). Tank 1 has volume $S_1(t) = pS(t)$, intercepts all inflow, $J(t)$, of age $T = 0$ across the vadose zone's upper boundary, and discharges to the next tank only its oldest water under plug flow sampling. Tank 2 has volume $S_2(t) = (1-p)S(t)$, receives only the oldest water from Tank 1, and selects water uniformly for discharge across the vadose zone's lower boundary. The transfer of water volume between tanks, $Q_\Delta(t)$ [L T^{-1}], is prescribed so as to ensure that water balance over the vadose zone is maintained.

$$Q_\Delta(t) = (1-p)J(t) + pQ(t) \tag{3}$$

The age-ranked storage function for the vadose zone as a whole is then the sum of the individual age-ranked storage functions for Tanks 1 and 2:

$$S_T(T,t) = S_{T1}(T,t) + S_{T2}(T,t) \tag{4}$$

It is easy to demonstrate that, when these two tanks are placed in series, the overall system conforms to a shifted-uniform SAS. The age distribution of water discharged from the vadose zone is the age distribution of water *discharged* from Tank 2 ($P_Q(T,t) = P_{Q2}(T,t)$) which, under uniform sampling, is equal to the age distribution of water *stored* in Tank 2. Therefore, from the definition of age-ranked storage (see equation (1a) and discussion thereof), the age distribution of water discharged from the vadose zone is the ratio of

the Tank 2 age-ranked storage function and the water volume stored in Tank 2 at any time t: $P_Q(T,t) = P_{Q2}(T,t) = \frac{S_{T2}(T,t)}{(1-p)S(t)}$. Substituting this result into the SAS closure relationship, $\Omega(S_T(T,t),t) = P_Q(T,t)$ (see equation 14 in Kim et al. (2016)), we obtain: $\Omega(S_T(T,t),t) = \frac{S_{T2}(T,t)}{(1-p)S(t)}$. Because all water in Tank 1 is younger than the youngest water in Tank 2, the age-ranked storage function for Tank 2 can be expressed as the difference between the overall age-ranked storage function, $S_T(T,t)$, and the volume of water stored in Tank 1 , $pS(t)$: $S_{T2}(T,t) = S_T(T,t) - pS(t)$ for $S_T(T,t) > pS(t)$. Combining these results we arrive at equation (2), proving that our tank-in-series model is mathematically equivalent to a shifted-uniform SAS for the vadose zone as a whole.

The age structure of water in Tanks 1 and 2 can be determined by solving the ACE separately for each tank, provided that the age distribution of water flowing out of Tank 1 equals the age distribution of water flowing into Tank 2. An important benefit of conceptualizing the problem in this way is that the ACE for each individual tank is linear, even though the ACE for the vadose zone as a whole is non-linear (i.e., the shifted-uniform SAS introduces non-linearity through the appearance of the dependent variable, $S_T(T,t)$, inside the Heaviside argument, see equation (2)). Because the ACE for each individual tank is linear, explicit solutions for each tank's age-ranked storage function can be derived, as described next.

2.1.2 Age-Ranked Storage in Tank 1

By transferring equation (1a) into the Laplace domain, the following solution for age-ranked storage in Tank 1 can be derived (Text 1, supplemental information):

$$S_{T1}(T,t) = \begin{cases} pS_0 - \bar{Q}_\Delta(t) + \bar{J}(t), \ T = T_0 + t \\ \bar{J}(t), \ t \le T < T_0 + t \\ \bar{J}(t) - \bar{J}(t-T), \ 0 \le T < t \end{cases} \qquad 0 \le t \le t_c \tag{5a}$$

$$S_{T1}(T,t) = \bar{J}(t) - \bar{J}(t-T), \quad 0 \le T \le T_{m1}(t), \quad t > t_c \tag{5b}$$

The new functions $\bar{J}(t)$ [L], $\bar{Q}(t)$ [L] and $\bar{Q}_\Delta(t)$ [L] represent the cumulative area-normalized volume of water, as of time t, added to the vadose zone by inflow, discharged from the

vadose zone, and transferred between Tanks 1 and 2, respectively:

$$\bar{J}(t) = \int_0^t J(\nu)\, d\nu \tag{6a}$$

$$\bar{Q}(t) = \int_0^t Q(\nu)\, d\nu \tag{6b}$$

$$\bar{Q}_\Delta(t) = (1-p)\bar{J}(t) + p\bar{Q}(t) \tag{6c}$$

The solution for age-ranked storage in Tank 1 takes on different functional forms depending on the choice of the age variable, T, and whether the elapsed time, t, is before or after a critical time, t_c [T]. The critical time is defined as the elapsed time at which all original water (i.e., water that was initially present in the vadose zone at time, $t = 0$) has been drained from Tank 1. It plays an important role in our solution by directly influencing the maximum age of water in Tank 1, which we denote by the variable $T_{m1}(t)$ [T]. In our two-tank representation of the vadose zone (Figure 1b), only the oldest water in Tank 1 (i.e., water with age $T_{m1}(t)$) is transferred from Tank 1 to Tank 2. Before the critical time, $t \leq t_c$, the oldest water in Tank 1 is original water. Because this original water is mathematically tagged with an age of T_0 at time $t = 0$ (see equation (1c) and discussion thereof), its age at any later time is: $T_{m1}(t \leq t_c) = T_0 + t$. After the critical time, $t > t_c$, an expression for the maximum age of water in Tank 1 can be derived by noting that, when the age variable is set equal to the maximum age, the age-ranked storage function must equal the total volume of water in Tank 1: $S_{T1}(T_{m1}(t), t) = S_1(t) = pS(t)$. Substituting equation (5b), we arrive at the following implicit solution for the maximum age of water in Tank 1 after the critical time:

$$pS(t) = \bar{J}(t) - \bar{J}(t - T_{m1}(t)),\ t > t_c \tag{7}$$

The critical time t_c, in turn, can be estimated directly from the vadose zone water balance, as the time required to drain all original water from Tank 1:

$$pS_0 = \bar{Q}_\Delta(t_c) \tag{8}$$

2.1.3 Graphical Interpretation of the Solution for Tank 1

Age-ranked storage can be represented graphically as a vertical water column with height equal to the area-normalized volume of water in storage, ordered by age from youngest at the top to oldest at the bottom (Figure 2). The age-ranked storage function for Tank

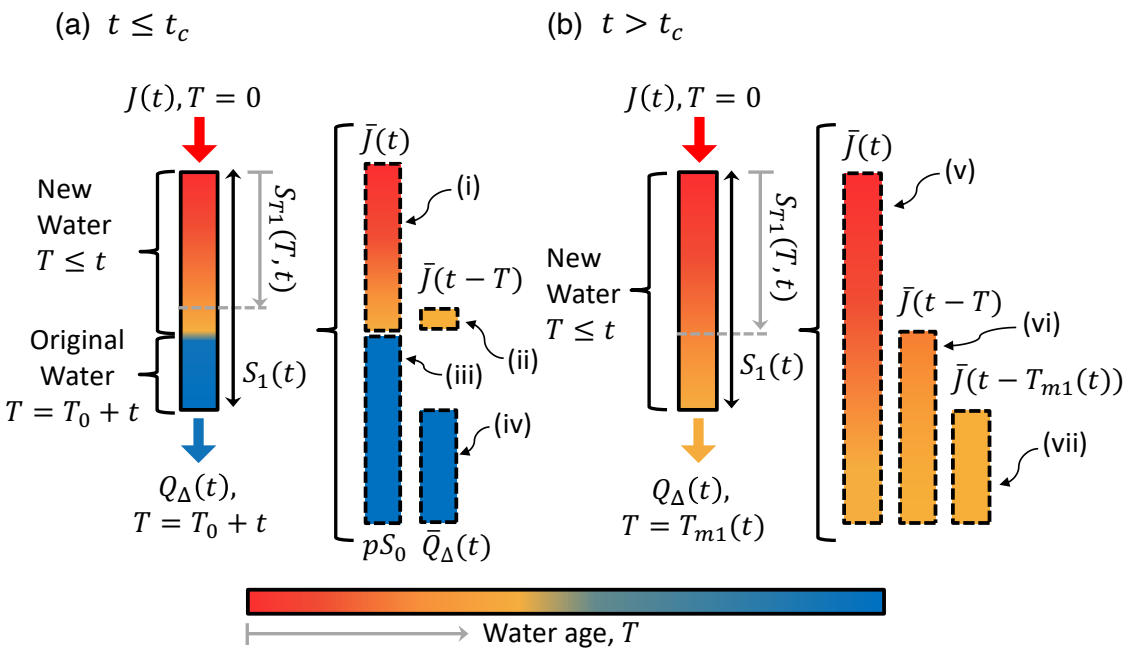

Figure 2: A graphical representation of the Tank 1 solution for age-ranked storage under plug flow sampling. The vertical columns with a solid border represent the total volume of water (per unit area) present in Tank 1 at any time t, $S_1(t) = pS(t)$. Age-ranked storage in Tank 1, $S_{T1}(T,t)$, is defined as the volume of water (per unit area) in Tank 1 storage of age T or younger at time, t (grey arrow). Cumulative and instantaneous flows are represented, respectively, with and without an overbar. (a) Prior to the critical time, $t \leq t_c$, the storage in Tank 1 consists of both original water (of age $T = T_0 + t$) and new water (of age $T < t$) that entered the vadose zone as inflow. The solution for age-ranked storage in this time range (equation (5a)) depends on four separate cumulative volumes represented graphically by vertical columns with dashed borders (labeled (i), (ii), (iii) and (iv)). (b) After the critical time, $t > t_c$, the storage in Tank 1 consists only of new water (of age $T < t$). The solution for age-ranked storage (equation (5b)) and implicit relationship for the maximum age (equation (7)) depend on three cumulative volumes (vertical columns with dashed borders labeled (v), (vi) and (vii)).

1, $S_{T1}(T,t)$, then represents the portion of storage in Tank 1 at time t with ages T or younger (gray vertical arrow in Figures (2a) and (2b)). Different functional forms for the Tank 1 age-ranked storage function apply before and after the critical time (equation (5a) and (5b), respectively) and depending on the choice of the age variable, T. Prior to the critical time t_c, the age-ranked storage function consists of three separate solutions that apply over different ranges of T (Figure 2a). When the age variable is set equal to the maximum age of water in storage, $T = T_0 + t$ (top solution in equation (5a)), age-ranked storage includes all water in Tank 1 storage, including all new water that flowed into the vadose zone up to time t (volume (i), Figure (2a)) plus the volume of original water that is still in Tank 1 (volume (iii) minus volume (iv), Figure (2a)). When the age variable falls in the range, $t \leq T < T_0 + t$ (middle solution in equation (5a)), the age-ranked storage function includes all new water that flowed into the vadose zone up to time t (volume (i), Figure (2a)). When the age variable falls in the range, $0 \leq T < t$ (bottom solution in equation (5a)), the age-ranked storage function includes only the portion of new water in storage with ages T or younger (volume (i) minus volume (ii), Figure (2a)).

Past the critical time, $t > t_c$, all original water has been discharged to Tank 2, and therefore Tank 1 storage consists only of new water (Figure (2b)). The corresponding solution for the Tank 1 age ranked storage function (equation (5b)) equals the total volume of new water that flowed into the vadose zone up to time t (volume (v), Figure (2b)), minus the portion of that new water that flowed into the vadose zone up to time $t - T$ (volume (vi), Figure (2b)).

A graphical interpretation can also be ascribed to the implicit solution for the maximum age of water in Tank 1 after the critical time (equation (7)). The total storage present in Tank 1 at time t (left hand side of equation (7) and solid bordered box in Figure (2b)) equals the cumulative volume of new water added up to time t (first term on the right hand side of equation (7) and volume (v) in Figure (2b)) minus the cumulative volume of new water added up to time $t-T_{m1}(t)$ (second term on right hand side of equation (7) and volume (vii) in Figure (2b)).

In summary, while the mathematics required to solve the ACE for Tank 1 are somewhat involved (Text 1 in supplemental information), the final result (equations (5a) and (5b)) can be easily understood graphically as a kinematic problem involving the inflow

and discharge of age-ranked water. Provided that the water balance over the vadose zone is known (i.e., time series for inflow $J(t)$, discharge $Q(t)$ and storage $S(t)$ are given), numerical implementation of the age-ranked storage function for Tank 1 involves three steps: (1) the critical time, t_c, is determined by solving for the root of equation (8); (2) for elapsed times less than the critical time, the maximum age of water in Tank 1 storage, $T_{m1}(t)$, is set equal to the sum of the initial age of original water plus elapsed time ($T_{m1}(t) = T_0+t$), while past the critical time the maximum age of water in Tank 1 storage is obtained for any elapsed time of interest by solving for the root of equation (7); and (3) with these results, the age-ranked storage function can be calculated from the algebraic expressions listed in equations (5a) or (5b).

2.1.4 Solution for Age-Ranked Storage in Tank 2

The solution for age-ranked storage in Tank 2 is as follows (derivation in Text 2, supplemental information):

$$S_{T2}(T,t) = \begin{cases} (1-p)S_0 e^{-\bar{\tau}(t)} + \int_0^t e^{-\bar{\tau}(t,\nu)} Q_\Delta(\nu)\, d\nu, \;\; T = T_0 + t \\ 0, \;\; 0 \le T < T_0 + t \end{cases} \qquad 0 \le t \le t_c \qquad (9a)$$

$$S_{T2}(T,t) = \begin{cases} (1-p)S_0 e^{-\bar{\tau}(t)} + \int_0^t e^{-\bar{\tau}(t,\nu)} Q_\Delta(\nu)\, d\nu, \;\; T = T_0 + t \\ \int_{t_c}^t e^{-\bar{\tau}(t,\nu)} Q_\Delta(\nu)\, d\nu, \;\; t \le T < T_0 + t \\ \int_{t_{i,2}(t-T)}^t e^{-\bar{\tau}(t,\nu)} Q_\Delta(\nu)\, d\nu, \;\; T_{m1}(t) \le T < t \\ 0, \;\; 0 \le T < T_{m1}(t) \end{cases} \qquad t > t_c \qquad (9b)$$

The new functions $\bar{\tau}(t)$ and $\bar{\tau}(t,\nu)$ represent discharge-weighted time over the time intervals $[0,t]$ and $[\nu,t]$, respectively.

$$\bar{\tau}(t) = \int_0^t \frac{Q(x)}{(1-p)S(x)}\, dx \qquad (10a)$$

$$\bar{\tau}(t,\nu) = \bar{\tau}(t) - \bar{\tau}(\nu) \qquad (10b)$$

Under steady-state hydrology, these expressions reduce to the ratio of elapsed time and the mean hydraulic residence time of Tank 2: $\bar{\tau}(t)$ and $\bar{\tau}(t,\nu) \rightarrow \frac{tQ_{ss}}{(1-p)S_{ss}}$ and $\frac{(t-\nu)Q_{ss}}{(1-p)S_{ss}}$, respectively, where the subscript "ss" denotes steady-state conditions.

The lower limit appearing in equation (9b), $t_{i,2}(t-T) = t_{i,2}(t_i)$, represents the elapsed time at which a water parcel entered Tank 2 from Tank 1, conditioned on the same water parcel entering the vadose zone at time $t_i = t - T$. An implicit expression

for $t_{i,2}(t-T)$ can be derived by noting that, after the critical time t_c, a water parcel entering Tank 2 at time $t_{i,2}$ must have entered the vadose zone (or Tank 1) at time, $t_i = t_{i,2} - T_{m1}(t_{i,2})$ (because Tank 1's plug flow SAS selects only the oldest water from storage for transfer to Tank 2). Likewise, a water parcel in Tank 2 with age T at time t must have entered the vadose zone (or Tank 1) at time, $t_i = t - T$. Equating these two vadose zone entrance times yields the following implicit relationship for the integral's lower-limit $t_{i,2}$:

$$t_{i,2} - T_{m1}(t_{i,2}) = t - T = t_i,\ t > t_c,\ T_{m1}(t) \leq T < t \tag{11}$$

A more formal derivation of this implicit solution for $t_{i,2}(t-T)$ is presented in Text 2 (supplemental information). According to equation (11), given a time series for the maximum age of water in Tank 1 storage ($T_{m1}(t)$, see equation (7)), the Tank 2 entrance time $t_{i,2}$ is solely a function of the time at which a water parcel entered the vadose zone across its upper boundary, t_i.

2.1.5 Graphical Interpretation of Solution for Tank 2

A graphical interpretation of the Tank 2 age-ranked storage function is presented in Figure 3. Prior to the critical time, $t \leq t_c$, water in Tank 2 consists solely of original water of age $T = T_0 + t$ (Figure 3a). This original water can be divided into the portion that was initially present in Tank 2 at time $t = 0$, $S_{0,2}(t)$, and the portion that was initially present in Tank 1 but transferred to Tank 2 over time t, $S_{0,1}(t)$. A solution for the function, $S_{0,2}(t)$, can be derived by noting that, under uniform sampling, the discharge rate of original water initially present in Tank 2 is proportional to both the total discharge rate, $Q(t)$, and the fraction of Tank 2 storage still occupied by that original water (Figure 3a):

$$\frac{dS_{0,2}}{dt} = \frac{S_{0,2}(t)}{(1-p)S(t)}Q(t) \tag{12}$$

Applying the initial condition, $S_{0,2}(t=0) = (1-p)S_0$, equation (12) can be integrated to yield the first term on the right hand side of the upper solution in equation (9a): $S_{0,2}(t) = S_0(1-p)e^{-\bar{\tau}(t)}$ (see lower portion of age-ranked storage in Figure 3a). Thus, the portion of original water that was initially present in Tank 2 at time $t = 0$ decays exponentially with discharge-weighted time.

A solution for the function, $S_{0,1}(t)$, can be derived by noting that the product $Q_\Delta(\nu)d\nu$ represents the differential volume of water transferred from Tank 1 to 2 over the time

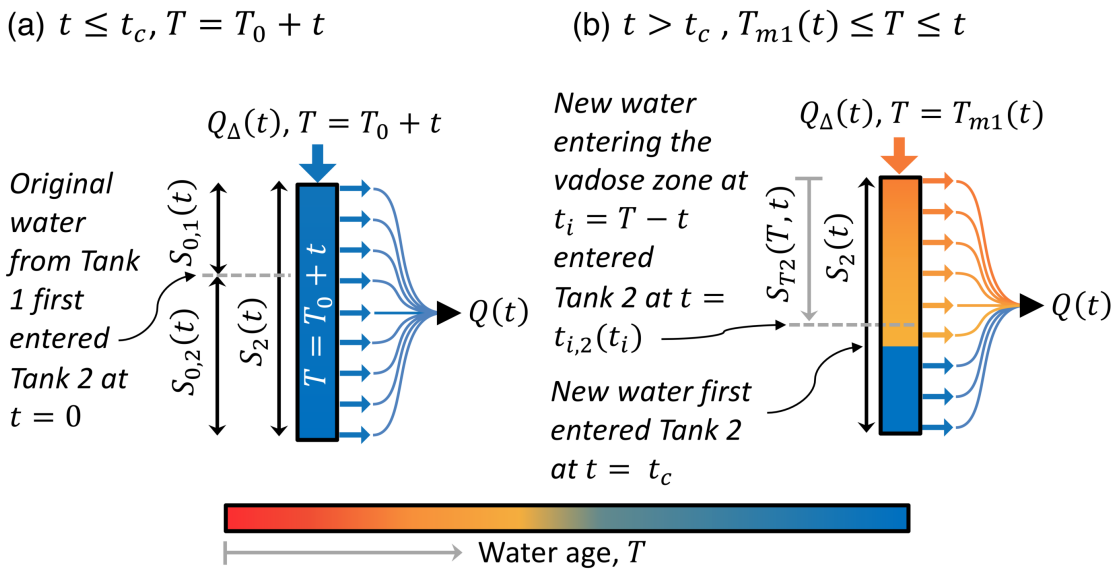

Figure 3: A graphical representation of the Tank 2 solution for age-ranked storage. (a) Before the critical time, only original water of age $T = T_0 + t$ is present in Tank 2 storage, including original water initially present in Tank 1 ($S_{0,1}(t)$) and original water that was initially present in Tank 2 ($S_{0,2}(t)$). (b) After the critical time, age-ranked storage in Tank 2 will always include some original water of age $T = T_0 + t$ (dark blue) plus new water that entered Tank 2 after elapsed time $t = t_c$. The time $t_{i,2}(t_i)$, which represents the Tank 2 entrance time of a water parcel that entered Tank 1 at time $t_i = t - T$, can be estimated by solving for the root of equation (11).

increment $d\nu$. Furthermore, by reference to the above solution for $S_{0,2}(t)$, following its introduction to Tank 2 at time ν, the portion of this differential volume of water remaining in Tank 2 will decay exponentially with discharge-weighted time, $dS_{0,1} = Q_\Delta(\nu)d\nu e^{-\bar{\tau}(t,\nu)}$. Integrating over all differential volumes of original water entering Tank 2 up to time t, we arrive at the second term on the right hand side of the upper solution in equation (9a): $S_{0,1}(t) = \int_0^t e^{-\bar{\tau}(t,\nu)} Q_\Delta(\nu)\, d\nu$. The boundary between $S_{0,1}(t)$ and $S_{0,2}(t)$ in Figure (3a) marks the location, in age-ranked storage, of the first parcel of original water that was transferred from Tank 1 to Tank 2 at time $t = 0$.

The bottom solution in equation (9a), $S_T(T < T_0 + t, t) = 0$ can be understood as follows. Prior to the critical time, all water in Tank 2 is original water. Therefore, by definition the age-ranked storage in Tank 2 is zero for any choice of the age variable less than the age of original water, $0 \leq T < T_0 + t$.

A similar line of reasoning can be used to derive the four separate solutions for age-ranked storage in Tank 2 after the critical time, $t > t_c$ (equation (9b) and Figure (3b)). The top solution in equation (9b) applies when the age variable is set equal to the maximum age of water in the vadose zone, $T = T_0 + t$. In this case, the age-ranked storage for Tank 2 includes all water in Tank 2 ($S_2(t)$ in Figure (3b)), including contributions from original water initially present in Tank 2 (first term on right hand side of equation (9b)) and all original and new water transferred into Tank 2 from Tank 1 up to time t (second term on right hand side of equation (9b)).

The second solution in equation (9b) applies when the age variable falls in the range $t \leq T < T_0 + t$. In this case the age-ranked storage function excludes all original water (of age $T = T_0 + t$) but includes all new water transferred into Tank 2 from Tank 1 of age $T \leq t$. The lower integration limit is therefore the critical time, t_c, when new water first entered Tank 2 from Tank 1 (Figure (3b)).

The third solution in equation (9b) applies when the age variable falls in the range $T_{m1}(t) \leq T < t$. In this case, age-ranked storage for Tank 2, $S_{T2}(T, t)$, includes only the portion of new water in Tank 2 that is of age T or younger at time t (i.e., the portion of age-ranked storage above the grey horizontal dashed line, Figure (3b)). The lower integration limit is therefore the Tank 2 entrance time, $t_{i,2}(t_i)$, of a water parcel that entered the vadose zone (or Tank 1) at time $t_i = t - T$ (see equation (11) and discussion thereof).

Finally, at time t all water in Tank 2 will be older than the maximum age of water in Tank 1, $T_{m1}(t)$. Therefore the Tank 2 age-ranked storage function is equal to zero for any choice of the age variable less than the maximum age of water in Tank 1 (fourth solution in equation (9b)).

Practical implementation of the age-ranked storage solution for Tank 2 entails four steps: (1) integrate equation (10a) to obtain a time series of discharge-weighted time, $\bar{\tau}(t)$, over the elapsed time interval [0,t]; (2) using the result from step (1), calculate the discharge-weighted time over any elapsed time interval [ν,t] (equation (10b)); (3) if the elapsed time of interest is past the critical time, find the root of equation (11) to obtain the elapsed time a water parcel enters Tank 2, $t_{i,2}(t_i)$, conditioned on the same water parcel entering the vadose zone at elapsed time, $t_i = t - T$; and (4) given the results from steps (1) through (3), numerically evaluate the appropriate solution for age-ranked storage depending on whether the elapsed time is before (equation (9a)) or after (equation (9b)) the critical time, and the choice of the age variable T.

2.2 Predicted Solute Breakthrough Concentration

2.2.1 Solute Breakthrough under Shifted Uniform Selection

The solute concentration leaving the vadose zone, $C_Q(t)$ [M L^{-3}], can be calculated from the foregoing results by convolving the solute concentration entering the vadose zone with new water, $C_J(t)$ [M L^{-3}], with the probability density function (PDF) form of the age distribution of new water leaving Tank 2, $p_{Q2}^{\text{new}}(T,t)$ [T^{-1}]:

$$C_Q(t) = \int_0^t C_J(t-T)\, p_{Q2}^{\text{new}}(T,t)\, dT, \;\; t > t_c \tag{13a}$$

$$p_{Q2}^{\text{new}}(T,t) = \frac{\partial P_{Q2}}{\partial T} = \frac{1}{(1-p)S(t)} \frac{\partial S_{T2}}{\partial T} \tag{13b}$$

Recall the term "new water" refers to water that entered the vadose zone across its upper boundary at some time $t > 0$ (in contrast to "original water" that was present in the vadose zone at time $t = 0$). Thus, the superscript "new" on the age distribution (equation (13b)) indicates that this is the age distribution of new water discharged from the vadose zone at any time t. Within the context of our model, new water cannot be discharged from the vadose zone until it enters Tank 2, which is why the upper limit on the convolution integral is restricted to elapsed times greater than the critical time, $t > t_c$. Combining equations (9b) and (13b) yields, after some manipulation (see Text 3, sup-

plemental information), the following solution for the PDF form of the age distribution of new water discharged from the vadose zone as a function of time t:

$$p_{Q2}^{\text{new}}(T,t) = \frac{J(t-T)}{(1-p)S(t)} e^{-\bar{\tau}(t,\, t_{i,2}(t-T))}, \;\; T_{m1}(t) \leq T < t, \;\; t > t_c \tag{14}$$

The lower bound on the age variable, $T_{m1}(t) \leq T$ is imposed because, as water is transferred from Tank 1 to 2 after the critical time, the oldest water in Tank 1 becomes the youngest water in Tank 2. The upper bound, $T < t$, is imposed because, as noted above, we are interested in the age distribution of new water discharged from the vadose zone, and by definition all new water entered the vadose zone for times, $t > 0$. Substituting the age distribution of new water discharged from the vadose zone (equation (14)) into the convolution integral (equation (13a)) we arrive at the following solution for the solute breakthrough concentration under shifted uniform selection:

$$C_Q(t) = \begin{cases} 0, \;\; 0 \leq t \leq t_c \\ \frac{1}{(1-p)S(t)} \int_0^{t-T_{m1}(t)} C_J(t_i) J(t_i) e^{-\bar{\tau}(t,\, t_{i,2}(t_i))} dt_i, \;\; t > t_c \end{cases} \tag{15}$$

The dummy integration variable, $t_i = t - T$, is the time a water parcel entered the vadose zone conditioned on it having age T at time t, and the function, $t_{i,2}(t_i)$, is the time that same water parcel entered Tank 2 (see equation (11) and discussion thereof).

2.2.2 Impulse-Response under Shifted-Uniform Selection

Under steady-state flow conditions, much can be inferred about a chemical reactor by observing its response to the impulsive application of a conservative tracer (Hill and Root (2014)). Here we demonstrate the same is true for an unsteady hydrologic system, at least one that is well-described by a shifted-uniform SAS. An impulsive input of solute to the vadose zone can be represented mathematically as follows: $C_J(t_i) = \frac{M''}{J(t_{\text{pulse}})} \delta(t_i - t_{\text{pulse}})$. Here, the variable t_{pulse} is the time at which the pulse entered the vadose zone with new water, the function $\delta(\cdot)$ is the Dirac Delta function and the variables M'' and $J(t_{\text{pulse}})$ represent, respectively, the mass per unit area and inflow entering the vadose zone at time, $t_i = t_{\text{pulse}}$. Substituting this expression into the shifted-uniform solution for solute breakthrough (equation (15)) we arrive at a remarkably simple expression for solute breakthrough, where discharge-weighted elapsed time, $\bar{\tau}(t, t_{\text{lag}})$, is given by equation (10b):

$$C_Q(t, M'', t_{\text{lag}}) = \begin{cases} 0, \;\; 0 \leq t < t_{\text{lag}} \\ \frac{M'' e^{-\bar{\tau}(t,\, t_{\text{lag}})}}{(1-p)S(t)}, \;\; t \geq t_{\text{lag}} \end{cases} \tag{16}$$

The new variable, t_{lag}, represents the time at which solute breakthrough begins; it is related to t_{pulse} through the implicit expression for the entrance time to Tank 2, where $T_{m1}(t)$ is the maximum age of water in Tank 1 at time t (see equations (7) and (11)):

$$t_{\text{lag}} - T_{m1}(t_{\text{lag}}) = t_{\text{pulse}} \tag{17}$$

In the event the pulse enters the vadose zone at time $t_{\text{pulse}} = 0$, the time lag reduces to the critical time, $t_{\text{lag}} = t_c$; i.e., the time at which all original water is drained from Tank 1 (see equation (8) and discussion thereof).

Equation (16) predicts that, following the impulsive addition of a conservative solute to an unsteady hydrologic system at time $t = t_{\text{pulse}}$, the breakthrough concentration is zero for $t < t_{\text{lag}}$. At $t = t_{\text{lag}}$, the breakthrough concentration increases from zero to $C(t = t_{\text{lag}}) = \frac{M''}{(1-p)S(t_{\text{lag}})}$, and thereafter declines more-or-less monotonically with discharge-weighted time (the inclusion of "more-or-less" here reflects the fact that, if storage were to decline, the breakthrough concentration could temporarily increase, all else being equal). The fraction p, which represents where along the plug flow to uniform sampling spectrum a particular hydrologic system falls, influences solute breakthrough in three ways, by appearing in: (1) the denominator on the right hand side of equation (16); (2) the definition of discharge-weighted time, $\bar{\tau}(t, t_{\text{lag}})$ (see equation (10b)); and (3) the expression for the maximum age of water in Tank 1 (see equation (7) which, in turn, influences the lag time (equation (17)). Using linear superposition, a solution can also be written for N pulses, where M_i'' and $t_{\text{pulse},i}$ are, respectively, the mass per unit area and input time for the i-th pulse:

$$C_Q(t) = \sum_{i=1}^{N} C_Q(t, M_i'', t_{\text{lag},i}) \tag{18a}$$

$$t_{\text{lag},i} - T_{m1}(t_{\text{lag},i}) = t_{\text{pulse},i} \tag{18b}$$

2.2.3 Solute Breakthrough under Plug Flow and Uniform Selection

We can also derive explicit expressions for solute breakthrough under pure plug flow and pure uniform sampling, corresponding to limits $p \to 1$ and 0, respectively. As outlined in supplemental information (Text 4), the predicted breakthrough solute concen-

tration under pure plug flow sampling is as follows:

$$C_Q^{\mathrm{PF}}(t) = \begin{cases} 0,\ 0 \le t \le t_c^{\mathrm{PF}} \\ C_J(t - T_m^{\mathrm{PF}}(t)), 0 \le T_m^{\mathrm{PF}} < t,\ t > t_c^{\mathrm{PF}} \end{cases} \tag{19a}$$

$$S_0 = \bar{Q}(t_c^{\mathrm{PF}}) \tag{19b}$$

$$S(t) = \bar{J}(t) - \bar{J}(t - T_m^{\mathrm{PF}}),\ \ t > t_c^{\mathrm{PF}},\ 0 \le T_m^{\mathrm{PF}} \le t \tag{19c}$$

The critical time at which all original water is drained from the vadose zone, t_c^{PF}, and the maximum age of water in storage after the critical time, $T_m^{\mathrm{PF}}(t)$ are given implicitly by the vadose zone water balance (equations (19b) and (19c), respectively).

Equation (20a) is the corresponding expression for solute breakthrough under uniform sampling (see Text 5 in supplemental information for derivation):

$$C_Q^{\mathrm{U}}(t) = \frac{1}{S(t)} \int_0^t C_J(t_i) J(t_i) e^{-\bar{\tau}^{\mathrm{U}}(t,t_i)}\, dt_i \tag{20a}$$

$$\bar{\tau}^{\mathrm{U}}(t, t_i) = \int_{t_i}^{t} \frac{Q(\nu)}{S(\nu)} d\,\nu \tag{20b}$$

3 Application to Solute Transport through the Vadose Zone

3.1 Experimental System and Unsteady Water Balance

As a first test of the above modeling framework, we turned to a previously published laboratory study of solute transport through an experimental model of a vadose zone with a perched water table (Kim et al., 2016). These experiments were conducted in a 1 m^3 sloping sand lysimeter irrigated twice per day for 28 days to simulate periodic rainfall events. Select rainfall events were spiked with chloride or deuterium tracers. The concentration of chloride and deuterium in water draining from the lysimeter (or tracer breakthrough curves) was measured over time at a nominal sampling frequency of 1 h^{-1}. Our model was applied to these data in three steps as follows. First, hourly estimates of discharge were calculated from hourly measurements of water storage (estimated from continuous measurements of the lysimeter's weight and fifteen frequency-domain reflectometry probes) and inflow to the lysimeter (measured with a magnetic flow meter): $Q(t) = J(t) - \frac{dS}{dt}$. Second, with the water balance in hand and knowledge of which irrigation pulses were spiked with either chloride or deuterium (at fixed concentrations of 6915 μ mol l^{-1} and 743.3 per mil, respectively), the two exact solutions for solute breakthrough under plug flow and uniform sampling (equations (19a) and (20a)) were numerically in-

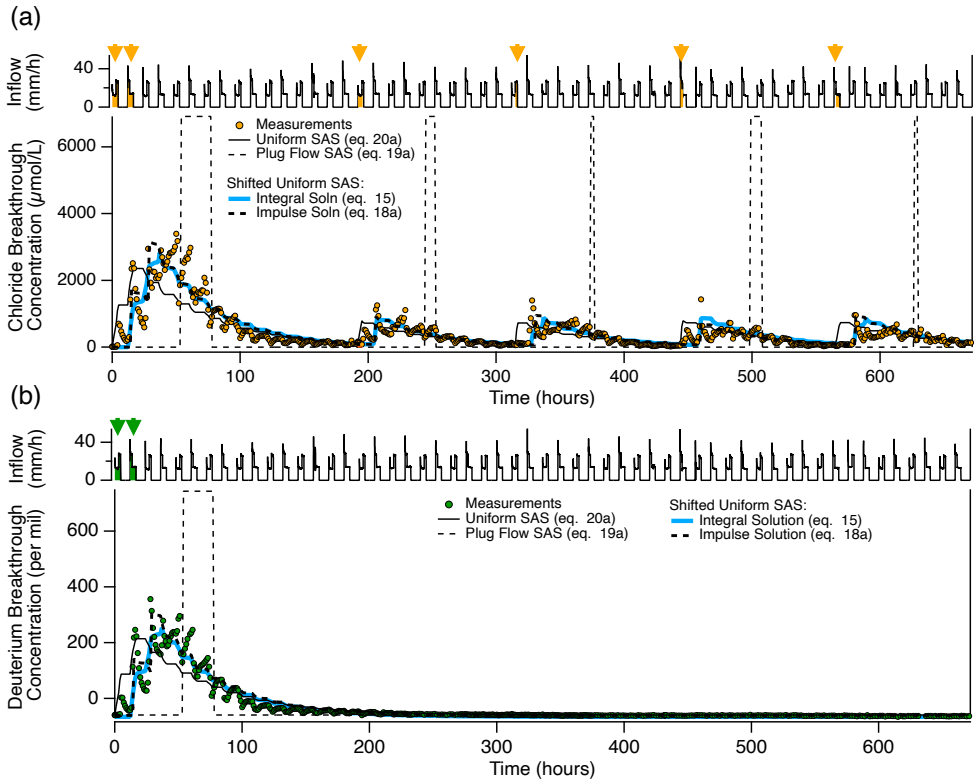

Figure 4: Comparison of measured and predicted breakthrough of either (a) chloride or (b) deuterium tracer in a model experimental hill slope system (bottom plots in each panel) subject to periodic irrigation (top plots in each panel) (data from Kim et al. (2016)). Predicted breakthrough concentrations are shown for plug flow sampling (thin dashed black curves), uniform sampling (thin solid black curves) and shifted uniform sampling with either the continuous solution (thick solid blue curve curves) or impulsive solution (thick dashed black curve). For the latter two simulations the inferred p values were 0.24 $\pm$0.05 and 0.23 $\pm$0.07 for, respectively, the chloride and deuterium breakthrough curves.

tegrated (Mathematica v.12, Wolfram Research, Inc.) to yield predicted breakthrough concentrations for the two tracers as a function of time. Third, to ascertain where along the plug flow-to-uniform sampling continuum Kim et al.'s experimental lysimeter falls, separate values for the fraction p were inferred from the chloride and deuterium breakthrough measurements by minimizing the root-mean-square-error (RMSE) between experimental data and breakthrough concentrations predicted by the shifted-uniform solution.

3.2 Testing the Integral Form of the Breakthrough Solution

The integral form of the shifted-uniform solution (equation (15)) closely tracks the breakthrough of both chloride and deuterium tracers over the 56 irrigation cycles monitored by Kim et al. (2016) (compare blue curve with orange and green circles, Figure 4). The inferred $p-$values (0.24 ± 0.05 and 0.23 ± 0.07, respectively), imply that at any given time roughly 24% of the youngest water is transiting through Tank 1, while 76% of the oldest water is uniformly sampled for discharge from Tank 2. Also shown in Figure 4 are model predictions for solute breakthrough in the limits of pure uniform and pure plug flow sampling. In the uniform sampling limit (equation (20a), thin solid black curve in Figure 4) model predicted solute breakthrough occurs prematurely (relative to the measured solute breakthrough) consistent with the fact that, in this limit, any solute entering the system is immediately subject to random sampling for discharge. In the plug flow sampling limit (equation ((19a), thin dashed black curve in figure 4), on the other hand, the predicted breakthrough curves are delayed between 17 and 39 hours (relative to the measured solute breakthrough) and the peak breakthrough tracer concentration equals the inflow tracer concentration. These last two observations can be explained by noting that, under pure plug flow sampling, solutes experience no spreading or dilution as they are transported through the control volume.

3.3 Testing the Impulsive Form of the Breakthrough Solution

In Kim et al.'s experiments, each tracer pulse was added to the irrigation water over some finite period of time. For the purposes of testing the impulsive model we can assume the tracer mass associated with each pulse was released all at once at the mid-point of the pulse. The mass per unit area for the i-th pulse was estimated as follows, $M_i'' = C_i \int_{t_{\text{start},i}}^{t_{\text{end},i}} J(\nu)\, d\nu$, where C_i is the concentration of the i-th pulse (assumed to be con-

Table 1: The timing and magnitude of Kim et al.'s chloride or deuterium pulses.

Pulse	t_{start}, h	t_{end}, h	t_{pulse}, h	t_{lag}, h	**Chloride**, M'', mole m^{-2}	**Deuterium**, M'', m
1	0	4.5	2.3	14.3	0.558	60.0
2	12	16.5	14.25	28.3	0.585	62.9
3	192	195	193.5	206	0.261	n.a.
4	315	316.5	315.8	330.2	0.263	n.a.
5	444	445.5	444.75	459	0.203	n.a.
6	565.5	568.5	567	580.7	0.273	n.a.

stant and equal to 6915 μ mol l^{-1} or 743.3 per mil for chloride or deuterium, respectively), $t_{\text{start},i}$ and $t_{\text{end},i}$ are the start and end times of the i-th pulse and $J(t)$ is inflow to the lysimeter. The timing of the i-th pulse was taken as: $t_{\text{pulse},i} = t_{\text{start},i} + \Big(t_{\text{end},i} - t_{\text{start},i}\Big)/2$. Values of M_i'' and $t_{\text{pulse},i}$ estimated for each chloride and deuterium pulse in Kim et al.'s experiments are summarized in Table 1. Substituting these values into equation (18a) and setting $p = 0.24$, we find that the predicted breakthrough curves for the impulsive solution (thick black dashed curves in Figure 4) closely track both the integral form of the breakthrough solution (blue curves) and the measured chloride and deuterium breakthrough measurements (orange and green circles). Compared to the integral solution, the impulsive solution often predicts a higher solute concentration just as the solute is first breaking through, consistent with the impulsive model's underlying assumption that all of the tracer mass enters the control volume at a single point in time. Indeed, the degree of concordance between the integral and impulsive breakthrough curves is remarkable considering the relatively small volume (1 m^3) of the experimental lysimeter utilized in Kim et al.'s study. Based on these results, the simple impulsive solution for solute breakthrough under shifted-uniform sampling (equation (18a)) may be sufficient for many practical applications.

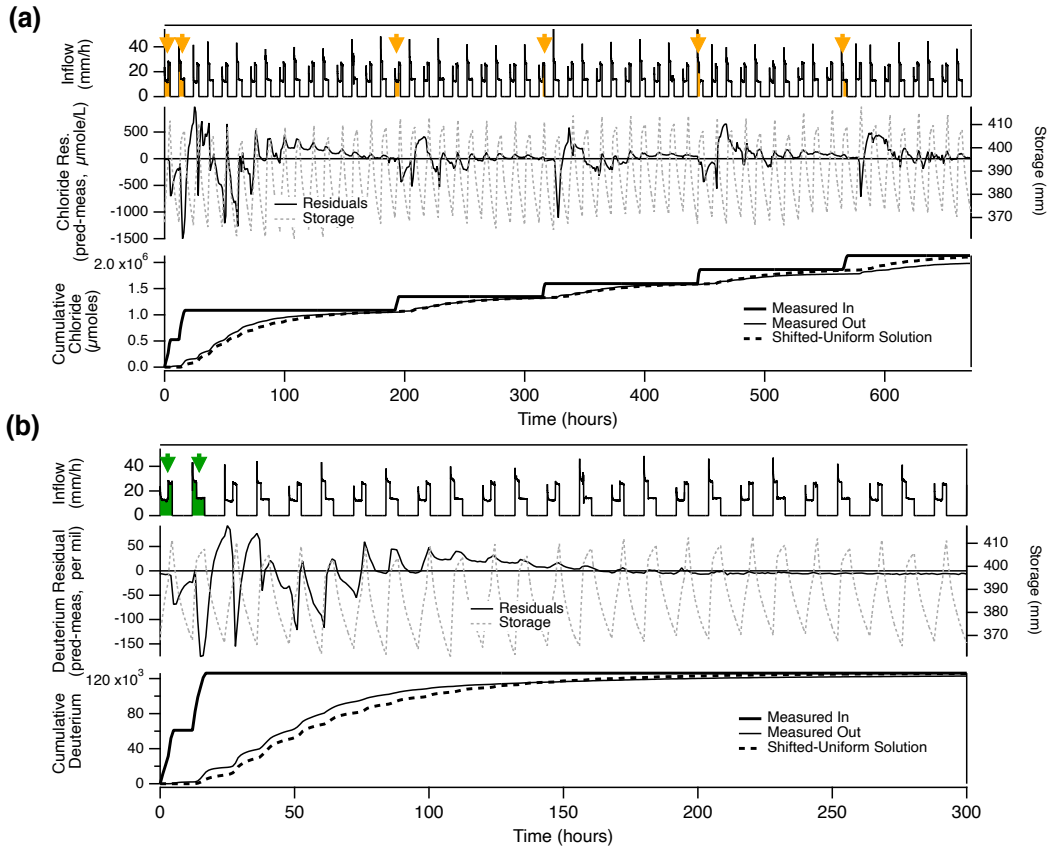

Figure 5: A comparison of (a) chloride and (b) deuterium model-data residuals (upper panel) and the cumulative mass entering and exiting the experimental system (lower panel). Residuals and predicted cumulative mass results were generated from the optimized shifted-uniform solution (blue curves in Figure 4).

3.4 Model Bias and the Inverse Storage Effect

An examination of the difference between predicted and measured breakthrough concentrations, or model residuals, reveals model bias at two timescales (Figure 5). Following the first two chloride and deuterium tracer pulses (time range 100 to 150 hours) breakthrough concentrations predicted by the shifted-uniform model consistently exceed measured values (i.e., the residuals are consistently positive). This long-period bias, which is also evident in Figure 4, could signal an underlying problem with the shifted-uniform SAS function or uncertainties associated with the overall volume balance. Relative to the latter, all three terms of the water balance (inflow, discharge and storage) were simultaneously measured by Kim et al. at an hourly time step, but errors in the discharge and irrigation rate measurements, along with unaccounted for evaporation and tank leakage, resulted in roughly 143 mm of "missing" water (personal communication). For our TTD analysis, we closed volume balance by calculating discharge from measured inflow and storage data, but in so doing may have introduced systematic biases in the volume balance that could account for these long-period positive residuals (e.g., by artificially concentrating solute discharged from the system).

A short period bias is also evident in Figure 5, that manifests as either negative or positive residuals during periods of high storage. Negative residuals occur at high storage immediately following the application of either chloride or deuterium tracers, while positive residuals occur at high storage in the intervals between tracer applications. This pattern indicates that the shifted-uniform SAS tends to under-sample young water during periods of high storage. That is, during periods of high storage following the application of a tracer-tagged pulse the solution tends to under-sample tracer-tagged water, while during periods of high storage following the application of a tracer-free pulse the solution tends to under-sample tracer-free water.

In their original analysis of these data, Kim et al. noted a similar pattern, whereby "younger water is released in greater proportion under wetter conditions than drier." This so-called inverse storage effect (ISE) appears to be associated with storage-dependent changes in the arrangement of, and partitioning between, internal flow pathways; for example, when water previously trapped in the unsaturated zone is mobilized as the water table rises during an irrigation event. In the context of our modeling framework, the ISE implies that the fraction p is not constant (as assumed here), but instead varies in-

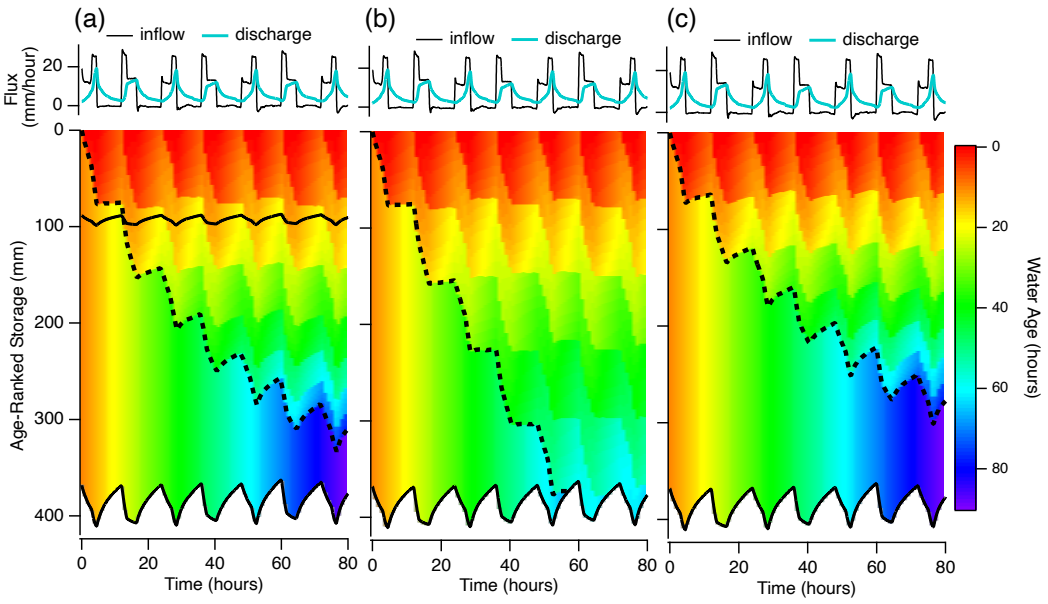

Figure 6: Age-ranked storage calculated from equations (5) and (9) during the first 80 hours of the lysimeter experiment under (a) shifted-uniform selection (assuming an optimized value of $p = 0.24$); (b) pure plug-flow selection ($p = 1$); and (c) pure uniform selection $p = 0$. The heavy black dashed curve in each panel denotes the boundary between new water (above the curve) and original water (below the curve). The lower black solid curve in each panel indicates total storage at any particular time. In panel (a), the upper solid black curve denotes the boundary between water stored in Tank 1 (above the curve) and Tank 2 (below the curve). For these simulations we marked original water with an initial age of $T_0 = 10$ hours.

versely with the volume of water present in storage, $S(t)$. Studies are presently underway to extend the shifted-uniform solution presented in this paper to account for the ISE. Even in its current form (with p constant), however, the shifted-uniform provides provides a very good first-order approximation of the measured solute breakthrough patterns (Figure 4) as well as the cumulative mass of solute discharged from the lysimeter over time (bottom panels, Figure 5a and 5b).

3.5 Time Evolution of Age-Ranked Storage

In addition to predicting solute transport through unsteady hydrologic systems (see last section), our solution for age-ranked storage under shifted-uniform selection (equa-

tions (5) and (9)) allows us to examine how the age structure of water in storage and outflow evolves over time (Figure (6a)). The thick dashed curve in each panel of this figure marks the boundary between original water that was present in the vadose zone at time $t = 0$ (below the curve) and new water that entered the vadose zone after $t = 0$ (above the curve). In these simulations we marked original water with an initial age of $T_0 = 10$ hours, and thus all age-ranked storage below the thick dashed curve ages linearly with time, $T = 10\text{h}+t$. The upper thin black curve in Figure (6a) represents the boundary between age-ranked water stored in Tank 1 (above the curve) and age-ranked water in Tank 2 (below the curve). Under plug flow sampling, only the oldest water in Tank 1 is selected for transfer to Tank 2. Consequently, original water in Tank 1 is progressively depleted until, at the critical time (t_c =12.6 hours), all original water has been transferred to Tank 2 and Tank 1 storage consists exclusively of new water (the critical time coincides with the cross-over of the upper solid curve and the thick dashed curve in Figure 6a). By contrast, under shifted-uniform selection original water is never entirely removed from Tank 2, although its proportion of Tank 2 storage declines over time. Because the total volume of water added to the vadose zone during each irrigation event is less than the average storage in Tank 1, a finite volume of water from the penultimate irrigation event is retained in Tank 1 during each irrigation cycle. This observation, together with the periodic irrigation schedule adopted for the experiment explains why, after the critical time, new water injected from Tank 1 into Tank 2 tends to be about 17 hours old (denoted by the orange color, Figure 6a). By the end of the 80 hour simulation, water discharged from the vadose zone is an approximately 1:3 mixture of original water with a single age of 90 hours and new water ranging in age from 20 to 70 hours (under shifted uniform sampling, the age distribution of water discharged from the vadose zone is equal to the age distribution of water stored in Tank 2, which in Figure (6a) corresponds to all age-ranked storage between the upper and lower solid black curves).

The predicted age distributions of water in the vadose zone in the plug-flow and uniform SAS limits are presented in Figures 6b and 6c, respectively. Under plug flow sampling only the oldest water stored in the vadose zone is selected for discharge, with the result that all original water is removed from the vadose zone by around 58 hours (denoted by the crossover of the thick dashed and solid curves near the bottom of Figure 6b). Compared to the shifted-uniform case described above, age-ranked storage in the plug-flow limit is substantially enriched in young water (compare Figures 6a and 6b).

In the uniform SAS limit, on the other hand, there is substantially more original water in storage at the end of the 80 hour simulation and the age distribution as a whole skews older (compare Figures 6a and 6c). This last result can be rationalized by noting that, in the uniform SAS limit, original water is removed from storage at a slower rate, all else being equal, because original water constitutes a smaller fraction of the total volume of water being uniformly sampled for discharge (see equation (12) and discussion thereof).

4 Discussion

4.1 Physical Interpretation of the Shifted-Uniform Solution

In this study we hypothesized that a shifted-uniform SAS might provide a first-order accurate assessment of mass transport through unsteady hydrologic systems. Application of the shifted-uniform solution to experimental measurements previously reported by Kim et al. (2016) supports this hypothesis with the caveat that, in its present form (i.e., with p constant) the model does not capture second-order effects associated with the storage-dependent rearrangement of internal flow paths. The relative success of the shifted-uniform solution begs the question: why does this simple model work so well?

One possible answer lies in the solution's series representation of two universal solute mass transport processes in porous media: advection along the fastest flow paths through a system (as represented by plug flow sampling of water and solute in Tank 1) and dispersive spreading and dilution (as represented by uniform sampling of water and solute in Tank 2). An estimate for the plug flow velocity through Tank 1, $v_1(t)$ [L T^{-1}], can be obtained from the ratio of the tank's depth, $pS(t)$, and the maximum age of water in the tank, $T_{m1}(t)$. Likewise, a dispersion coefficient for Tank 2, $D_2(t)$ [L^2 T^{-1}], can be estimated by dividing the mean residence time in Tank 2, $\mu_2(t)$ [T], into the square of the tank's depth, $(1-p)S(t)$.

$$v_1(t) = \frac{pS(t)}{T_{m1}(t)} \tag{21a}$$

$$D_2(t) = \frac{(1-p)^2 S^2(t)}{\mu_2(t)} \tag{21b}$$

$$\mu_2(t) = \frac{S_0}{S(t)} t e^{-\bar{\tau}(t)} + \frac{1}{(1-p)S(t)} \int_0^t (t-u) Q_\Delta(u) e^{-\bar{\tau}(t,u)}\, du \tag{21c}$$

The expression adopted here for the mean residence time in Tank 2 (equation (21c)) is the mean age of water in Tank 2 assuming that: (1) water entering the tank has an age

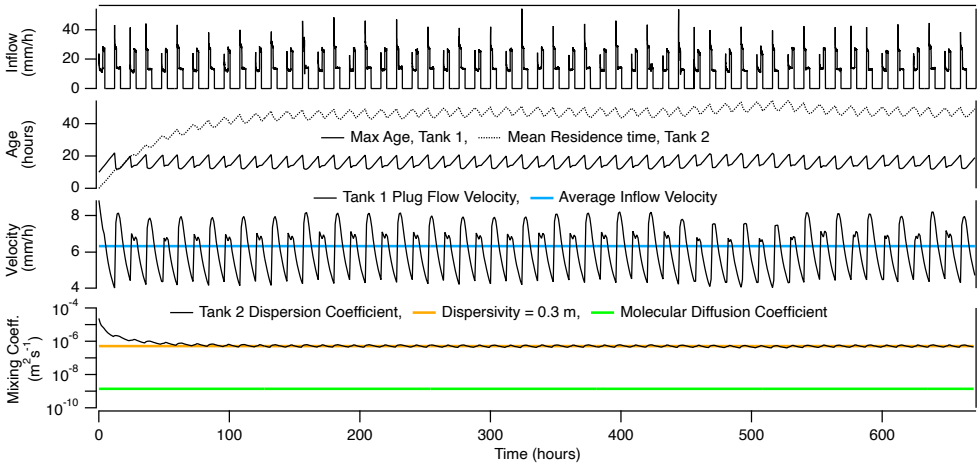

Figure 7: A physical interpretation of the shifted-uniform solution as applied to tracer transport through a model experimental vadose zone, including inflow timeseries (top graph), maximum age and mean residence time of water in Tanks 1 and 2 (second graph), implied plug flow velocity through Tank 1 (third graph) and implied dispersion coefficient in Tank 2 (fourth graph).

of $T = 0$h and (2) water initially present in the tank at time $t = 0$ has an age of $T_0 =$ 0h (compare with equation (7c) in Parker et al. (2021)).

When these formulae are applied to Kim et al.'s data (Figure 7), we find that, after a start-up period of roughly 100 hours, the maximum age in Tank 1 (equation (7)) and the mean residence time in Tank 2 (equation (21c)) fluctuate around 15.9 ± 2.7 and 47.6 ± 2.3 hours, respectively. The plug flow velocity estimated from equation (21a) (6.1 ± 1.2 mm h^{-1}) closely approximates the average infiltration rate into the lysimeter (6.7 ± 9.6 mm h^{-1}), consistent with our hypothesis that plug flow sampling of water and solutes in Tank 1 represents advective transport through the lysimeter. The dispersion coefficient inferred from equation (21b) (5.1 ± 0.53×10^{-7} m^2 s^{-1}) is roughly 370 times larger than the molecular diffusion coefficient for chloride in water at 25°C (2.03×10^{-9} m^2 s^{-1}) (Rumble (2022)). When the inferred dispersion coefficient is divided by the average discharge velocity from Tank 2 (6.31 ± 3.82 mm h^{-1}) the resulting dispersivity (0.29 ± 0.18 m) is within the range, although at the high end, of values reported previously for sandy media over similar transport distances (O(1m)) (Gelhar et al. (1992)), not accounting for source dispersion which is likely operating here as well (Kim et al. (2016)). Thus, as

hypothesized, uniform sampling from Tank 2 approximates solute spreading through the vadose zone by mechanical and source dispersion. In summary, the apparent success of the shifted-uniform solution likely stems from its series representation of two universal mass transport mechanisms, including advection along fast flow paths (Tank 1) and spreading by mechanical (kinematic) and source (geomorphic) dispersion (Tank 2).

4.2 Capturing Evapotranspiration and Age-Dependent Reactions

The exact solutions presented above for age-ranked storage and solute breakthrough can be amended to include evapotranspiration, conditioned on some theory for how water selected for ET is biased by age. For example, if plant roots preferentially sample the oldest water in vadose zone storage (as might occur at the end of a wet season, see Figure 6b in Hrachowitz et al. (2016)) it may be appropriate to incorporate ET as an additional outflow mechanism from Tank 2 under plug flow selection (which removes only the oldest water in storage). Following the same solution procedure outlined above for Tank 1 (see Section 2.1.2), this can be accomplished mathematically by setting the age distribution of water leaving by ET equal to, $P_{ET} = H(T - T_{m2}(t))$, where $T_{m2}(t)$ [T] is the maximum age of water in Tank 2 as a function of time. As with Tank 1, the maximum age in Tank 2 will be equal to the age of original water, $T_{m2}(t) = t + T_0$, up until a critical time for Tank 2, t_{c2} [T]. After the critical time, the maximum age in Tank 2 is determined from the following implicit expression, which follows from the fact that the age ranked storage in Tank 2, evaluated at $T = T_{m2}(t)$, must equal the total storage in Tank 2: $S_{T2}(T_{m2}(t), t) = (1 - p)S(t)$.

Likewise, our solution for solute breakthrough under shifted-uniform selection can be easily amended to capture age-dependent reactions, by letting the input concentration, $C_J(t_i = t - T, T)$, encode both the time at which the solute of interest entered the vadose zone (as reflected in the functional dependence on t_i), as well as how the nonconservative solute either increases or decreases with age as it transits through the system of interest (as reflected in the functional dependence on T): $C_Q(t) = \int_0^t C_J(t_i = t - T, T) p_{Q2}^{\text{new}}(T, t) dT$ where $t > t_c$ (compare with equation (13a)).

5 Conclusions

Unsteady TTD theory provides a powerful approach for understanding, and predicting, the transport and transformation of solutes through complex and time-varying natural and engineered hydrologic systems. At its core, the theory assumes that water leaving a hydrologic system is composed of a collection of water parcels of different ages that all reached the system outlet at the same time, and were consequently combined to yield the observed solute concentration discharged from the system. In the context of TTD theory, the "combining process" is carried out by the SAS function, which stipulates how the sampling of water in storage for outflow is biased by age. As noted by Hrachowitz et al. (2016), the SAS function therefore integrates two universal transport mechanisms that control solute transport and transformation in environmental matrices: (1) where and when a solute enters the system, which determines along which flow path the solute transits through the system (source or geomorphic dispersion) and (2) local variation in flow velocities along any particular flow path (kinematic or mechanical dispersion). Put another way, the SAS function is an emergent property of the physics (and depending on context, chemistry and biology) governing solute transport through a particular system, although general rules for its selection in practice remain elusive.

In this paper we propose and test what we call a shifted-uniform SAS, as a possible generic first-order description of solute transport through unsteady hydrologic systems. This SAS function, which can be represented conceptually and mathematically by two-tanks in series, captures the combined influence of geomorphic and kinematic dispersion by imposing a storage-dependent minimum transit time through the system (upstream tank under plug flow sampling) and then randomly sampling the water and solutes that pass through the first step for outflow (downstream tank under uniform sampling). The SAS function's single parameter, p, determines how water stored in the system at any given time is partitioned between the upstream and downstream tanks, and thus where a particular hydrologic system falls along the plug-flow ($p \to 1$) to uniform ($p \to 0$) sampling continuum. In addition to providing a compelling conceptual framework, the two tank representation of the shifted-uniform SAS also opens the door to the derivation of explicit formulae for the age-structure of water in storage (equations (4), (5) and (9)) and outflow (equation (5)), and for the solute breakthrough concentration under both continuous (equation (15)) and impulsive (equation (18a)) solute loading to the system.

Fitting equation (15) to previously published breakthrough measurements of chloride and deuterium in a sloping lysimeter subject to periodic wetting, we obtain an optimized value of about $p = 0.24$. The implied range of advective velocities and dispersivities (in Tanks 1 and 2, respectively) are very close to what we would expect for this experimental vadose zone (see Figure 7 and discussion thereof). It is important to stress that, although the shifted-uniform SAS is time-invariant, the residence time distribution of water in storage and the age distribution of water in outflow are both strongly time varying, as is evident from the predicted age-ranked storage in Tanks 1 and 2 over the first 80 hours of the lysimeter's operation (Figure 6a). Indeed, a weakness of the shifted-uniform SAS in its current form is precisely its time-invariance, specifically its inability to account for the enrichment of young water in outflow during periods of high storage. Allowing the fraction p to vary inversely with storage might address this so-called inverse storage effect, and efforts are currently underway to explore this possibility.

Acknowledgments

The authors declare no conflict of interest. SBG was supported by a U.S. National Science Foundation Growing Convergence Research Program award (NSF Award 2021015) and Virginia Tech's Charles E. Via, Jr. Department of Civil and Environmental Engineering; CH was supported by a U.S. National Science Foundation grant (NSF Award EAR-1654194). SBG and CH developed the modeling framework, SBG drafted the manuscript, both co-authors contributed edits. The miniLEO data is available in Hydroshare; see Kim et al. (2021).

References

Allen, R., Pereira, L., Raes, D., & Smith, M. (Eds.). (1998). *Crop evapotranspiration–guidelines for computing crop water requirements–fao irrigation and drainge paper 56.* Washington D.C., U.S.A.: Food and Agriculture Organization of the United Nations.

Benettin, P., Rinaldo, A., & Botter, G. (2013). Kinematics of age mixing in advection-dispersion models. *Water Resources Research*, *49*, 8539-8551. doi: https://doi.org/10.1002/2013WR014708

Botter, G., Beertuzzo, E., & Rinaldo, A. (2011). Catchment residence and travel time distributions: The master equation. *Geophysical Research Letters*, *38*,

L11403. doi: https://doi.org/10.1029/2011GL047666

Botter, G., & Rinaldo, A. (2003). Scale effect on geomorphologic and kinematic dispersion. *Water Resources Research*, *39*, 1286. doi: https://doi.org/10.1029/2003WR002154

Gelhar, L., Welty, C., & Rehfeldt, K. (1992). A critical review of data on field-scale dispersion in aquifers. *Water Resources Research*, *28*, 1955-1974. doi: https://doi.org/10.1029/92WR00607

Haber, A., Nugroho, S., & Taha, A. (2021). Control node selection algorithm for nonlinear dynamic networks. *IEEE Control Systems Letters*, *5*(4), 1195-1200. doi: https://doi.org/101109/LCSYS.2020.3019591

Hester, E., & Fox, G. (2020). Preferential flow in riparian groundwater: Gateways for watershed solute transport and implications for water quality management. *Water Resources Research*, *56*, e2020WR028186. doi: https://doi.org/10.1029/2020WR028186

Hill, C., & Root, T. (Eds.). (2014). *Introduction to chemical engineering kinetics and reactor design, second edition.* Hoboken, New Jersey, U.S.A.: John Wiley Sons, Inc.

Hrachowitz, M., Benettin, P., van Brekelen, B. M., Fovet, O., Howden, J., Nicholas, Ruiz, L., ... Wade, A. J. (2016). Transit times-the link between hydrology and water quality at the catchment scale. *WIREs Water*, *3*, 629-657. doi: https://doi.org/10.1002/wat2.1155

Kim, M., Pangle, L. A., Cardoso, C., Lora, M., Volkmann, T. H., Wang, Y., ... Trock, P. A. (2016). Transit time distributions and storage selection functions in a sloping soil lysimeter with time-varying flow paths: Direct observation of internal and external transport variability. *Water Resources Research*, *52*, 7105-7129. doi: https://doi.org/10.1002/2016WR018620

Kim, M., Volkmann, T. H. M., Wang, Y., Meira Neto, A. N., Katarena, M., Harman, C. J., & Troch, P. A. (2021). Biosphere 2 Landscape Evolution Observatory 2016 PERTH experiment - Dataset for the LEO east and west hillslopes. *HydroShare*. doi: 10.4211/hs.a74168d3396c436a8f0cd5910358df13

Kirchner, J. W. (2016). Aggregation in environmental systems–part 1: Seasonal tracer cycles quantify young water fractions, but not mean transit times, in spatially heterogeneous catchments. *Hydrology and Earth Systems Science*, *20*,

279-297. doi: https://doi.org/10.5194/hess-20-279-2016

Parker, E., Grant, S., Cao, Y., Rippy, M., McGuire, K., Holden, P., & et. al. (2021). Predicting solute transport through green storm water infrastructure with unsteady transit time distribution theory. *Water Resources Research*, *57*, e2020WR028579. doi: https://doi.org/10.1029/2020WR028579

Rinaldo, A., Benettin, P., Harman, C. J., Hrachowitz, M., McGuire, K. J., van der Velde, Y., ... Botter, G. (2015). Storage selection functions: A coherent framework for quantifying how catchments store and release water and solutes. *Water Resources Research*, *51*, 4840-4847. doi: https://doi.org/10.1002/2015WR017273

Rinaldo, A., Marina, A., & Rigon, R. (1991). Geomorphological dispersion. *Water Resources Research*, *27*, 513-525. doi: https://doi.org/10.1029/90WR02501

Rodriguez, N. B., McGuire, K. J., & Klaus, J. (2018). Time-varying storage-water age relationships in a catchment with a mediterranean climate. *Water Resources Research*, *54*, 3988-4008. doi: https://doi.org/10.1029/2017WR021964

Rumble, J. (Ed.). (2022). *Handbook of chemistry and physics, 102nd edition.* Boca Raton, Florida, U.S.A.: CRC Press.

Simunek, J., van Genuchten, M., & Sejna, M. (2008). Development and applications of the hydrus and stanmod software packages and related codes. *Vadose Zone Journal*, *7*(2), 587-600. doi: https://doi.org/10.2136/vzj2007.0077